Original

Effect of tempering time on the ballistic performance of a high strength armour steel

Pradipta Kumar Jena*, Ponguru Senthil P., Siva Kumar K.

Defence Metallurgical Research Laboratory, Kanchanbagh, Hyderabad 500 058, India

Abstract

The investigation describes and analyses the effect of tempering time on the mechanical and ballistic performance of a high strength armour steel. The steel is subjected to tempering at 300 °C for 2, 24 and 48 h. A marginal variation in strength and hardness is observed with increase in tempering time, whereas ductility and Charpy impact values are found to be decreasing. Ballistic performance of the samples are evaluated by impacting 7.62 mm and 12.7 mm armour piercing projectiles at 0° angle of impact. Results show a small variation in the ballistic performance when impacted with 7.62 mm armour piercing projectile. A decrease in ballistic performance of the material is observed with increasing tempering time when impacted with 12.7 mm armour piercing ammunition.

1. Introduction

Suitable material selection is very crucial with respect to reduction in weight of armour and it is essential to determine the material with lowest possible areal density for a defined threat. Many high strength steels, aluminium alloys and titanium alloys are being used as armour. Amongst them high strength steels are predominantly used for armour applications owing to their low cost, superior mechanical properties, good machinability and high performance. Ballistic performance of metallic materials depends on parameters like strength, hardness, toughness, microstructure, strain hardening rate, etc. An optimization of these material properties against projectile impact has long been of practical interest in military applications. Some previous studies showed that ballistic performance largely depends on the hardness of the material.

Dikshit, Kutumbrao, and Sundararajan (1995) found that under plain strain condition the ballistic resistance increases linearly with hardness of the steel. But, under plane stress conditions optimum ballistic performance is observed at an intermediate hardness level. In another study on the ballistic testing of 50CrV4 steel, it was pointed out that with increase in hardness of the target plate the penetration ability of the projectile decreases significantly (Ubeyli, Yildirim, & Ogel, 2007). Maweja and Stumpf (2008a, 2008b) found that the microstructure and the ratio of yield to tensile strength had a significant influence on the ballistic behaviour of armour steels. In a recent study on the ballistic behaviour of different high strength steels by Borvik, Dey, and Clausen (2009), it was demonstrated that there is a linear increase in perforation resistance with yield stress. Srivathsa and Ramakrishnan (1999) formulated ballistic performance maps for thick metallic armour target plates, and indicated that ballistic performance is a strong function of strain-hardening rate. In a previous study it was shown that ballistic performance does not depend on any specific independent parameter. Instead, an optimized value of all the parameters like strength, hardness, toughness leads to the best ballistic performance (Jena et al., 2010).

Heat treatment is the commonly used process to develop desired properties in steels. Of all the microstructures produced by heat treatment, martensite forms the highest level of strength in steels. However, because of large internal stresses

---

* Corresponding author.

E-mail addresses: pradipta_rrlb@rediffmail.com, pradipta@drdo.ac.in (P.K. Jena).

Peer Review under the responsibility of Universidad Nacional Autónoma de México.

Table 1
Chemical composition of the steel.

Material	Chemical composition
DMR 1700 steel	0.35–0.44% C, 0.45–055% Mn, 1.8–2.2% Si, 0.8–1.2% Cr, 2.5–3.4% Ni, 0.45–0.55% Mo, 0.25–0.35% Co, 0.01% P, 0.01% S, Balance Fe

associated with the martensitic transformation, martensite phase is rarely used in an untempered condition. Tempering increases the ductility and toughness in steels, which are essential for enhancing impact energy absorption. In tempering two parameters, namely, temperature and time, play vital roles in determining the mechanical properties of the steel. A considerable amount of work has been carried out to understand the effect of tempering temperature on the mechanical properties of steel (Demir, Übeyli, & Yıldırım, 2008; Jena, Ramanjeneyulu, Sivakumar, & Bhat, 2009; Lee & Su, 1999; Malakondaiah, Srinivas, & Rao, 1997). These studies reflect that the temperature employed for tempering is limited because of the loss of strength resulting from the high tempering temperatures. Temper embrittlement is another factor restricting the choice of temperature. Hence it is of interest to explore the effect of tempering time. Only limited studies on the effect of tempering time on the properties of steel are reported in open literature. In one of the earlier works, Lee and Su (1999) found that there is a slight decrease in strength and hardness with increase in tempering time. However, it was observed that ductility increases with increase in tempering time.

2. Material and experimental procedure

DMR-1700 steel is a medium carbon high strength armour steel. Previous studies on this steel showed that 300 °C tempering temperature gives maximum strength (Malakondaiah et al., 1997). But the Charpy impact values obtained at this tempering temperature are not high. The low Charpy impact values are the contributions of the residual stresses at 300 °C tempering temperature. Charpy impact toughness is an important parameter which contributes to the ballistic performance (Jena et al., 2010). So it is aimed in this study to explore the effect of increased tempering time on mechanical properties including Charpy impact values and ballistic performance of DMR-1700 steel.

The steel was made by vacuum arc melting in Mishra Dhatu Nigam Limited, India. It was supplied in the form of 50 mm thick rolled plates. The nominal chemical composition of the steel is given in Table 1. Samples of 150 mm × 150 mm × 50 mm were cut from a single plate and subjected to heat treatment. For the present tests, the austenitisation temperature was 925 °C and the tempering temperature was 300 °C. The samples were first austenitised for 2 h followed by quenching in oil. The plates were immediately tempered for 2 h, 24 h and 48 h followed by cooling to room temperature in air. Austenitizing and tempering were carried out in a neutral atmosphere furnace.

Small samples were cut from the heat-treated plates and subjected to standard metallographic examination. The specimens were etched at room temperature using 2% Nital (2 ml HNO₃,
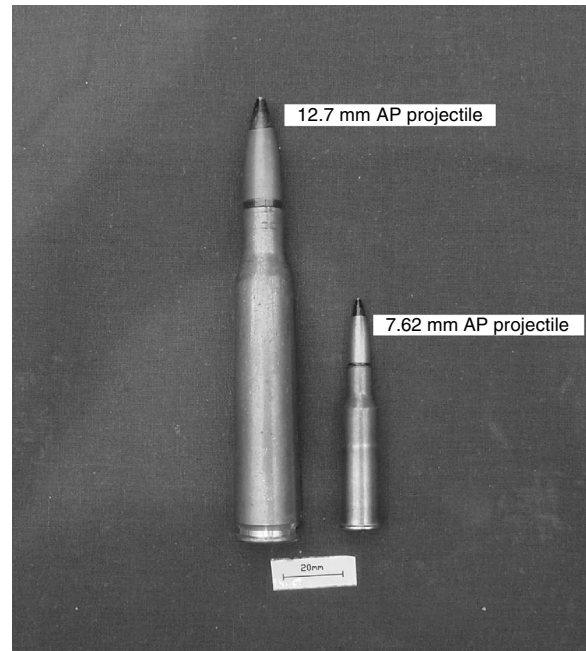

Fig. 1. Photographs of the two different armour piercing projectiles used for the present study.

and 98 ml Methyl Alcohol) to reveal the microstructure. Optical and scanning electron microscope (SEM) was used to observe the microstructure of the heat-treated plates. Following metallographic observations, the bulk hardness of the target plates were measured according to ASTM E 140-02 using an AFFRI Vickers hardness tester under 30 kg applied load for 15 s. The average hardness of a particular sample was reported from measurements over 10 locations.

Cylindrical tensile specimens were machined from the heat treated plates in the longitudinal orientation of the rolled plate. The size and geometry of the specimens as well as the testing procedure are in accordance with ASTM E8-93. Tests were done at a strain rate of $4.8 \times 10^{-1} \, s^{-1}$ using an Instron Universal Testing machine (Instron 5500R) to determine the mechanical properties. Three samples for each heat treated condition were prepared and tested at room temperature. Standard Charpy V-notch (2 mm deep notch) specimens (10 mm × 10 mm × 55 mm size) were also machined as per the ASTM standards (E23-02a) and the tests were carried out using the Tinius-Olsen impact testing instrument to find out the impact properties. The weight of the hammer used in the impact test was 27.3 kg. Five samples of each heat treatment were tested and the average value was taken as the impact value of plates for that heat treatment. Following the Charpy impact testing, the fracture surfaces of broken impact specimen were also carried out. The topographical features were observed by using a LEO scanning electron microscope operated at 20 kV.

Heat treated steel plates were impacted with 2 different non-deformable armour piercing steel projectiles. Fig. 1 presents the general views of the projectiles. Table 2 gives more detailed description of the projectiles. The angle of attack was normal to the target plates. The striking velocity of the projectiles was measured using infrared light emitting diode photovoltaic cell

Table 2
Some properties of the projectiles.

Type	Property	
	7.62 AP	12.7 AP
Cartridge length	70.88 ± 0.48 mm	147.3 ± 0.2 mm
Cartridge material	Copper	Copper
Jacket material	Soft steel	Soft steel
Core material	High hardness steel	High hardness steel
Bullet length	26.53 mm	52.7 mm
Diameter of high hardness projectile	6.06 mm	10.75 mm
Nose type	Conical	Conical
Core weight	5.342 g	30.049 g
Jacket weight	4.849	17.813
Total bullet wt (core weight + jacket wt)	10.375 g	48.424 g
Bullet weight with brass jacket	22.781 g	129.47 g
Striking velocity	820 ± 10 m/s	850 ± 10 m/s
Kinetic energy	1.796 kJ	10.85 kJ

by measuring the time interval between the interceptions caused by the projectile running across two transverse beams placed 2 m apart. The projectiles were fired from a distance of 10 m. The testing arrangement is also given elsewhere (Jena et al., 2009). Three shots were fired on each plate and three sets of plates of each heat treatment were fired in order to get the ballistic behaviour statistically. The average penetration value was taken as the ballistic performance of the plate. Following impact and penetration, damage patterns at the front face of the target plates were investigated.

3. Results

3.1. Microstructure

Fig. 2 shows the optical micrographs of the steel at differently tempered conditions. All the heat-treated steel samples show tempered martensitic structure. Scanning electron micrographs are taken to further examine the microstructural changes at different tempered conditions, Fig. 3. From SEM micrographs it is observed that in all the tempered cases the martensitic lath size and grain size are more or less similar.

3.2. Mechanical properties

The mechanical properties of the steel samples at different tempering conditions are evaluated and the representative engineering stress–strain curves and true stress–strain curves are depicted in Fig. 4. It can be seen that the strength and hardness values are similar at all the tempered conditions, Fig. 5(a). A marginal increase in strength and hardness is observed with increasing the tempering time. However, there is a gradual decrease in ductility measured in terms of percentage elongation with increase in tempering time, Fig. 5(b). There is a significant effect of tempering time on the Charpy impact values of the
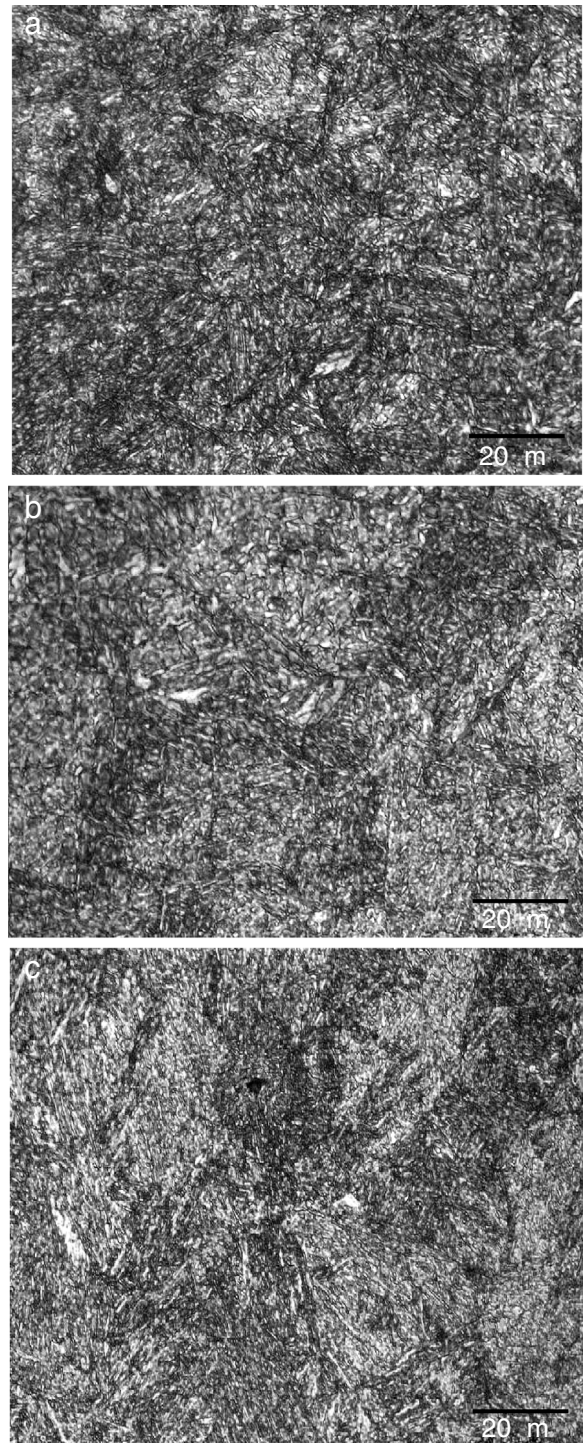

Fig. 2. Optical microstructure of (a) 2 h tempered sample, (b) 24 h tempered sample and (c) 48 h tempered sample.

steel, Fig. 5(b). The impact toughness of the steel substantially decreases with increase in tempering time.

3.3. Fractography

Scanning electron microscopic observations are made at the fracture surface of the Charpy impact samples to identify the mode of fracture as a function of tempering time, Fig. 6. In the
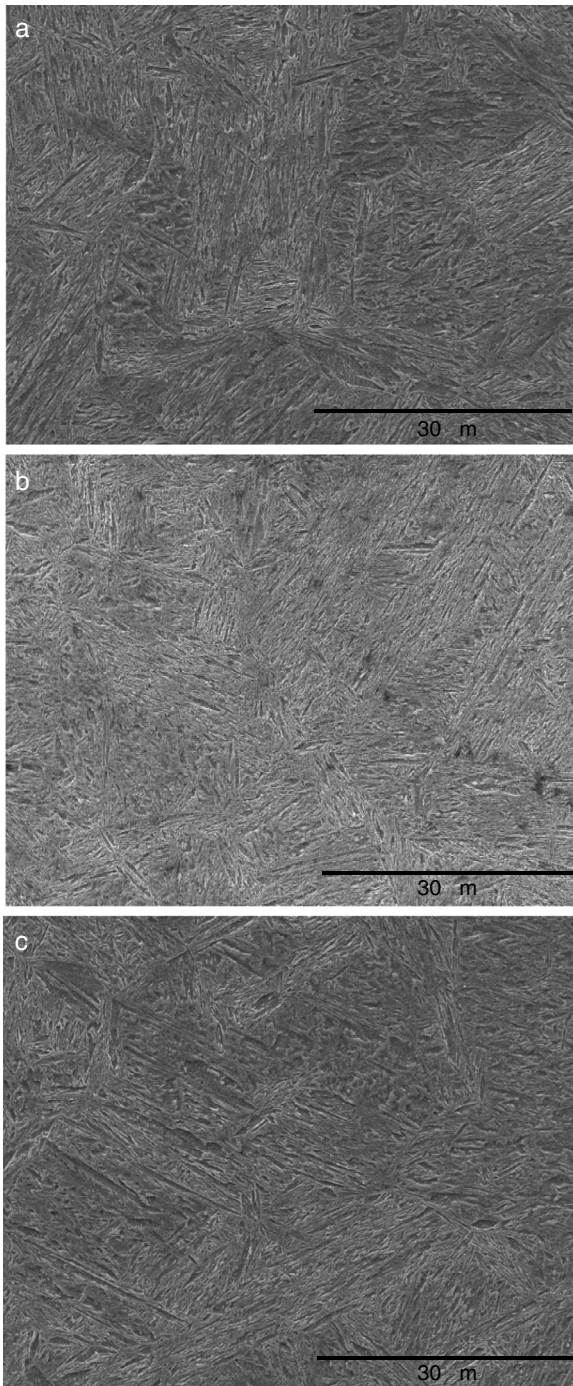
Fig. 3. Scanning electron micrographs of (a) 2 h tempered sample, (b) 24 h tempered sample and (c) 48 h tempered sample.
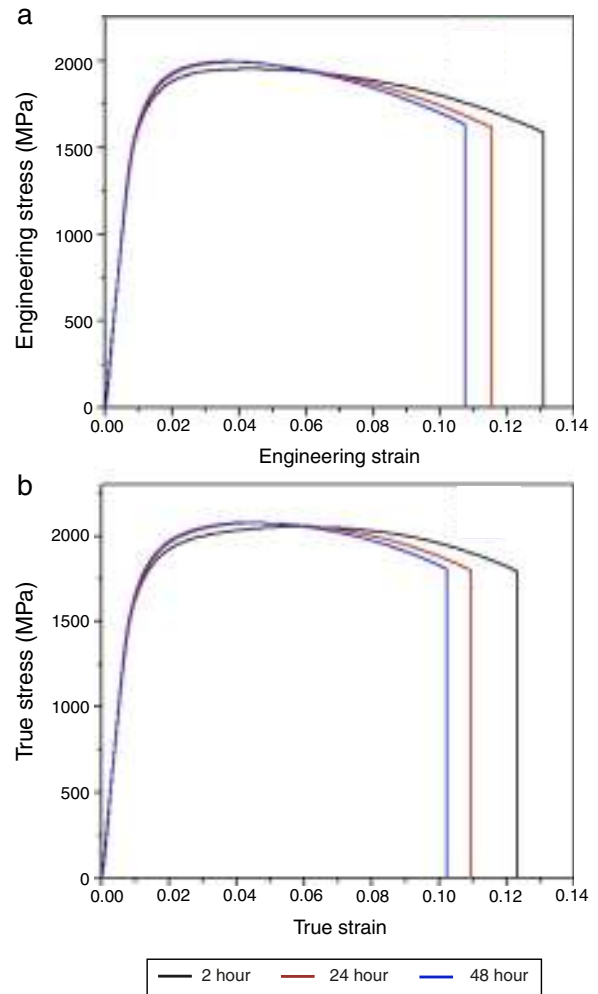

Fig. 4. (a) Engineering stress–strain curves for the differently heat treated plates. (b) True stress–strain curves for the differently heat treated plates.

3.4. Ballistic testing

Ballistic performance of all the samples was measured using the depth of penetration (DOP) method described elsewhere (Jena et al., 2010). The DOP of all the samples are measured and are plotted against tempering time, Fig. 7. It can be seen that there is only a small variation in DOP in case of 7.62 AP projectiles. However in case of 12.7 AP projectiles there is a significant variation in DOP with tempering time. The DOP increases beyond 2 h of tempering. The average DOP of the 2 h tempered sample against 12.7 mm AP projectile is measured to be 14.2 mm, whereas it is 16.3 mm and 18.1 mm respectively in 24 h and 48 h tempered samples.

Fig. 8 shows a close view of the front face of the samples ballistically evaluated against 7.62 AP projectiles. The craters are almost similar in appearance. However, small cracks are observed inside of the crater wall in 24 h and 48 h tempered samples. But no such cracks are observed in case 2 h tempered samples.

Fig. 9 shows cut views of the craters in the target plates tempered at 48 h and impacted by 7.62 AP as well 12.7 AP projectiles. As can be seen the crater formed by 7.62 AP projectiles

2 h tempered specimens, ductile fracture mechanism is dominant as shown in Fig. 6(a). This dimple like morphology clearly indicates a ductile failure mode and the progress of damage following a void nucleation, growth and coalescence process. However, the fracture surface of the specimens tempered at 24 h and 48 h shows presence of quasi cleavage features along with dimples, which suggests a mixed mode fracture behaviour at higher tempering time, Fig. 6(b). The dimple size is also coarser than that in the case of 2 h tempered specimens.
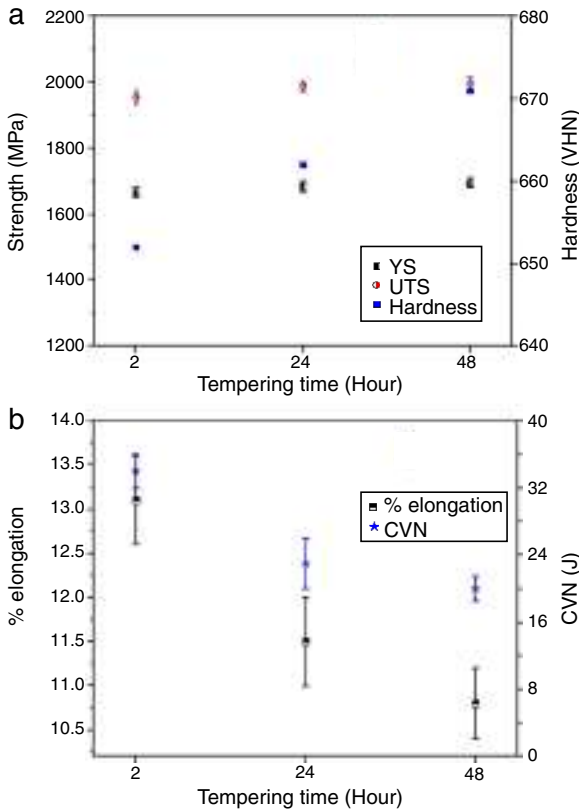
Fig. 5. (a) Variation in strength and hardness with tempering time. (b) Variation in percentage elongation and impact toughness with tempering temperature.

is considerably smaller to that of the crater formed by 12.7 AP projectiles. The average crater diameter formed by 7.62 AP projectiles is found to be approximately 12 mm where as the average crater diameter formed by 12.7 AP projectiles is measured to be approximately 25 mm. The crater volume is measured by filling the crater up to the original target plate level with plasticine of known density (Dikshit, 1998). It is found that the average volume of the crater formed by 7.62 AP projectiles is measured to be 412 mm^3 where as the average volume of the crater formed by 12.7 AP projectile is found to be 2620 mm^3.

4. Discussion

As per Hollomon and Jaffe the tempering parameter is $T(c + \log t)$, where 'T' is the temperature equal to $^\circ$F + 460, 't' is the time in hours and 'c' a constant for a particular steel (Hollomon & Jaffe, 1945). Grange and Baughman used the tempering parameter to formulate isohardness graphs which indicate equal hardness levels of tempered martensite with varying combinations of temperature and time during tempering (Grange & Baughman, 1956). This means a particular hardness level of the tempered martensite can be achieved by different combinations of time and temperature. Grange and Baughman found that a value of 18 for the constant 'c' holds good for majority of the steels. Using the tempering parameter other combinations of tempering temperature and time have been calculated which match the studied tempering temperature and time. From the calculations it is found that tempering the steel at 300 $^\circ$C for
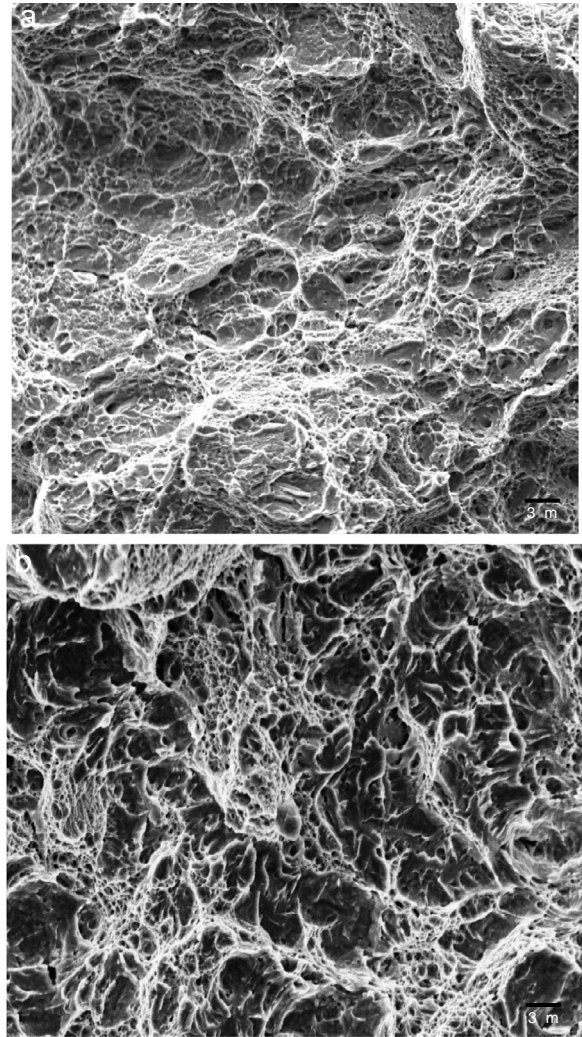

Fig. 6. SEM fractographs of the broken Charpy impact samples. (a) 2 h tempered sample. (b) 48 h tempered sample.
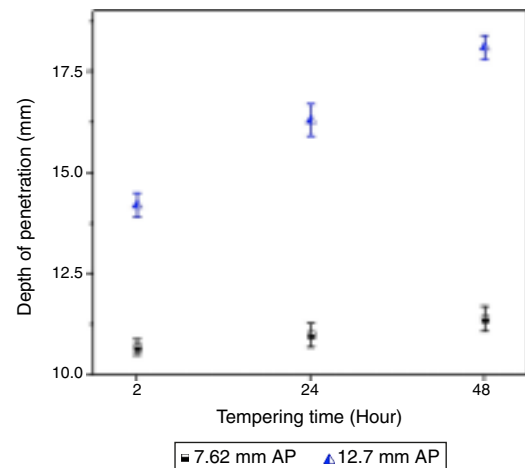

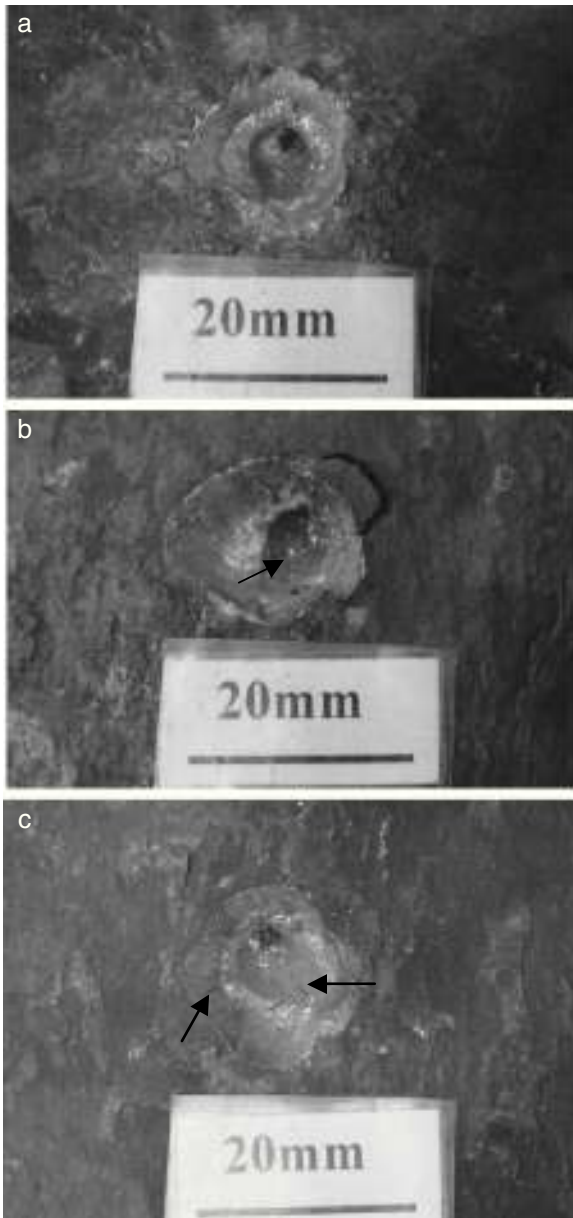Fig. 7. Effect of tempering time on ballistic performance of target plates.

Fig. 8. Top view of the craters after ballistic impact against 7.62 AP ammunition. Small cracks are pointed out by arrow marks in the crater in 24 h and 48 h tempering target plates. (a) 2 h impacted sample. (b) 24 h impacted sample. (c) 48 h impacted sample.

24 h and 48 h matches with tempering the steel at 361 °C for 2 h and 378 °C for 2 h respectively. Tempering time is taken 2 h in the calculations, so that all the differently tempered samples can be compared on the basis of equivalent temperature only.

Loss in toughness after tempering at 300 °C for 24 h and 48 h suggests occurrence of temper martensite embrittlement, which occurs due to the formation of interlath carbide films due to the decomposition of retained austenite (Lee & Su, 1999; Malakondaiah et al., 1997; Sarikaya, Jhingan, & Thomas, 1991). So it can be inferred that increasing the tempering time has led to a heat-treatment condition where the steel is susceptible to temper martensite embrittlement (TME). This is well matched with the fracture surface observation of the higher tempering
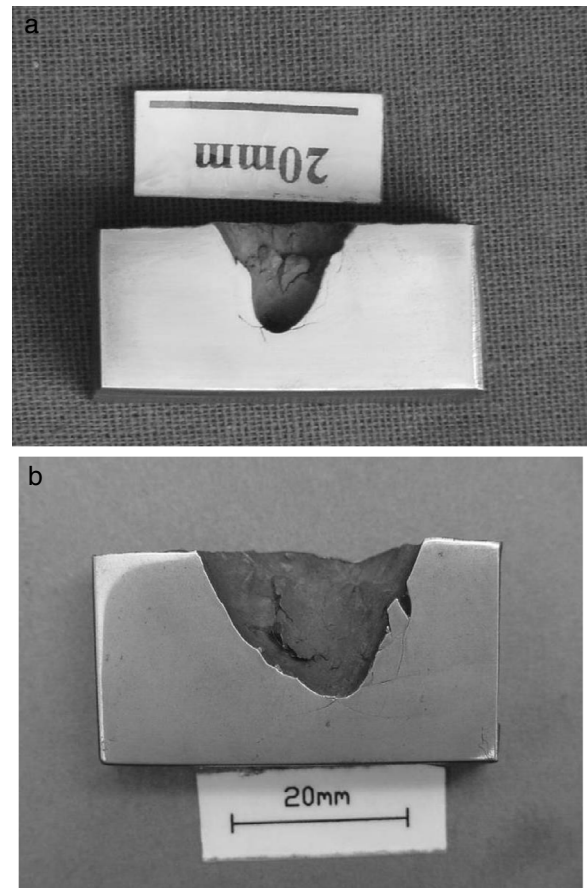

Fig. 9. Crater cut views of the 48 h tempered samples impacted against. (a) 7.62 mm AP projectile and (b) 12.7 mm AP projectile.

time Charpy impact samples, Fig. 7. This is again well supported from the observation of cracks in the crater surface of 24 h and 48 h tempered samples, Fig. 8. A previous study on DMR 1700 steel has also documented the drop in impact toughness around 350 °C tempering (Jena, Sivakumar, & Bhat, 2007).

When projectile strikes, the kinetic energy of the projectile is transferred to the target plate. The kinetic energy (KE) of the 7.62 mm projectile and 12.7 mm projectiles are calculated according to the formula

$$KE = \frac{1}{2}mv^2 \tag{1}$$

where m is mass of the projectile, v is velocity of the projectile. The KE values of the two projectiles are given in Table 2. Only the mass of the steel core is taken for calculating the KE of the projectiles, because the soft jacket gets readily deformed and does not cause any significant additional damage to the target plate. It can be seen that the 7.62 mm projectile carries almost 6 times lesser kinetic energy than that of 12.7 mm projectile while the volume of the holes created is nearly 5 times smaller. Hence the kinetic energy passed on to the unit volume of the interacting material is also smaller for 7.62 AP projectiles.

There are two principal parameters which control the ballistic performance of the target material. First, the strength parameters which determine energy absorption during deformation

and second, toughness parameters which determine the energy absorption during fracture. Higher toughness of the material measured in terms of Charpy impact energy, enables absorption of higher amount of energy during the terminal fracturing process.

In the case of larger 12.7 mm AP projectile, as compared to 7.62 mm AP projectile more kinetic energy is imparted per unit volume of the armour material. The 2 h tempered material with a higher Charpy impact value is able to better dissipate the kinetic energy during the fracturing while due to lower Charpy impact values the 24 h and 48 h tempered samples absorb lower amounts of energy during fracturing of the material leading to lowered ballistic performance in spite of UTS and hardness remaining nearly similar.

5. Conclusion

Increase in tempering time leads to an embrittlement domain and hence reduced the toughness of the studied steel tempered at 300 °C. In case of 7.62 mm AP projectiles, hardness and strength of the material are important for ballistic performance. In 12.7 mm AP projectiles apart from strength and hardness, the Charpy impact value plays a significant role in determining the ballistic performance. Therefore studies on ballistic performance of materials against lower calibre projectiles cannot be extended for larger calibre projectiles even at similar velocities.

Conflict of interest

The authors have no conflicts of interest to declare.

Acknowledgement

References

Borvik, T., Dey, S., & Clausen, A. H. (2009). Perforation resistance of five different high-strength steel plates subjected to small-arms projectiles. *International Journal of Impact Engineering*, *36*, 948–964.

Demir, T., Übeyli, M., & Yıldırım, R. O. (2008). Investigation on the ballistic impact behavior of various alloys against 7.62 mm armor piercing projectile. *Materials and Design*, *29*, 2009–2016.

Dikshit, S. N., Kutumbrao, V. V., & Sundararajan, G. (1995). The influence of plate hardness on the ballistic penetration of thick steel plates. *International Journal of Impact Engineering*, *2*, 293–320.

Dikshit, S. N. (1998). Ballistic behaviour of tempered steel armour plates under plane strain conditions. *Defence Science Journal*, *48*(2), 167–172.

Grange, R. A., & Baughman, R. W. (1956). Hardness of tempered martensite in carbon and low alloy steels. *ASM Transactions*, *48*, 165–197.

Hollomon, J. H., & Jaffe, L. D. (1945). Time tempering relations in tempering steels. *Transactions, American Institute of Mining and Metallurgical Engineers, 162*, 223.

Jena, P. K., Mishra, B., Ramesh Babu, M., Babu, A., Singh, A. K., Sivakumar, K., et al. (2010). Effect of heat treatment on mechanical and ballistic properties of a high strength armour steel. *International Journal of Impact Engineering*, *37*, 242–249.

Jena, P. K., Ramanjeneyulu, K., Sivakumar, K., & Bhat, T. B. (2009). Ballistic studies on layered structures. *Materials and Design*, *30*(6), 1922–1931.

Jena, P. K., Sivakumar, K., & Bhat, T. B. (2007). Effect of heat treatment on mechanical and ballistic properties of ultra high strength DMR-1700 steel. *Metals Materials Process*, *19*(1–4), 339–346.

Lee, W. S., & Su, T. T. (1999). Mechanical properties and microstructural features of AISI 4340 high-strength alloy steel under quenched and tempered conditions. *Journal of Materials Processing Technology*, *87*, 198–206.

Malakondaiah, G., Srinivas, M., & Rao, P. R. (1997). Ultra high strength low alloy steels with enhanced fracture toughness. *Progress in Materials*, *42*, 209–242.

Maweja, K., & Stumpf, W. (2008a). The design of advanced performance high strength low carbon martensitic armour steels, microstructural considerations. *Materials Science and Engineering A*, *480*, 160–166.

Maweja, K., & Stumpf, W. (2008b). The design of advanced performance high strength low carbon martensitic armour steel. Part 1. Mechanical property considerations. *Materials Science and Engineering A*, *485*, 140–153.

Sarikaya, M., Jhingan, A. K., & Thomas, G. (1991). Retained austenite and tempered martensite embrittlement in medium carbon steels. *Material Science and Engineering A*, *132*, L5–L9.

Srivathsa, B., & Ramakrishnan, N. (1999). Ballistic performance maps for thick metallic armour. *Journal of Material Processing Technology*, *96*, 81–91.

Ubeyli, M., Yildirim, R. O., & Ogel, B. (2007). On the comparison of the ballistic performance of steel and laminated composite armors. *Materials and Design*, *28*(4), 1257–1262.